Real-Time Thermal Characterization of Power Semiconductors using a PSO-based Digital Twin Approach

Johannes Kuprat[1], Yoann Pascal[2], Marco Liserre[1]
[1] Chair of Power Electronics, Kiel University, Kaiserstrasse 2, 24143 Kiel, Germany
[2] Fraunhofer Institute for Silicon Technology ISIT, Fraunhoferstr. 1, 25524 Itzehoe, Germany
Phone: +49 (0) 431-880 6105
Fax: +49 (0) 431-880 6103
Email: jk@tf.uni-kiel.de, yoann.pascal@isit.fraunhofer.de, ml@tf.uni-kiel.de
URL: https://www.pe.tf.uni-kiel.de

Keywords

≪Modelling≫, ≪Thermal Model≫, ≪Optimization≫, ≪Diagnostics≫.

Abstract

Thermal impedance is essential for assessing the state-of-health of power semiconductors and to use thermal observers. This work proposes a Particle-Swarm-Optimization-based Digital Twin approach to extract the thermal impedance for online monitoring. A proof of concept of the approach is achieved in a real-time simulation with a digital reference model by showing the convergence to the given parameter set. Further, the convergence of the algorithm to a fixed parameter set is validated in the laboratory.

Introduction

The field of power electronics is of utmost importance due to its necessity for the integration of renewable energy sources and electric vehicle charging stations into the electrical grid [1]. A relevant topic in the field of power electronics is the reliability of the devices [2], especially the one of semiconductors and capacitors [3]. The thermal characteristics of the devices are a keystone for assessing their state-of-health via condition monitoring [4] and to use thermal observers [5] as well as active thermal control [6].

The concept of Digital Twins (DTs) is of growing relevance for academia and industry [7]. There are various definitions of DTs [7], in this work a DT refers to a real-time digital replicate of a physical system, which takes into account measurements and historical data to optimize the accuracy of the digital model. Recently, different approaches for the implementation of DT replicating the electrical behavior of power electronic converters have been proposed, which are based on Particle-Swarm-Optimization (PSO) [8], neural networks [9], polynomial chaos expansion [10], and bayesian optimization [11]. Prior, real-time thermal simulations have been proposed for reliability evaluation [12–16].

Furthermore, [17] proposed using DT approaches for the description of the converter reliability and [18] implemented a real-time thermal DT based on an extended Kalman filter. However, the demonstrated thermal DT was implemented with the assumption of temperature measurements at all nodes of the equivalent circuit, so the problem is decoupleable and the algorithm optimizes only one RC element of a Cauer network for each pair of temperature measurements. However, this does not enable to access also not measurable temperatures within power semiconductor modules. This work proposes a PSO-based DT approach for thermal real-time identification, which is capable of optimizing up to three RC elements of a Cauer network with only one pair of temperature measurements (Fig. 1).

This work is structured as follows: the proposed PSO-based thermal DT approach is introduced in the next section. Afterwards, the results of the Real-Time Simulation (RTS) with a digital reference model

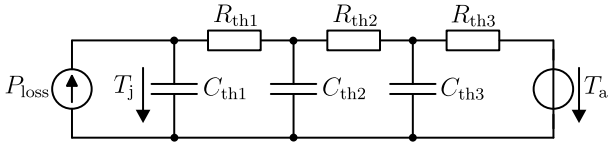

Fig. 1: Thermal modeling between junction and case temperature by a Cauer network with three RC elements.

are presented. Then the performance of the DT on the laboratory setup is shown. Thereafter, critical topics for the implementation of the PSO-based thermal DT in field applications are discussed. At the end the conclusion of the work is given.

PSO-based Thermal Digital Twin Approach

The PSO-based thermal DT is a RTS of a physical converter which is executed in parallel to its real operation. The PSO optimizes the thermal model based on measurements of junction and ambient temperatures (T_j and T_a) on the physical converter. As shown in Fig. 2, the PWM signals given by a Digital Signal Processor (DSP) are provided to the physical converter, which is in this case a buck converter, and to the electrical RTS of this buck converter at the same time. The voltage and current of this electrical RTS are then used to calculate the switching and conduction losses based on look-up tables, which also depend on the measured T_j. The estimated losses and the measured T_a are the inputs for the thermal RTSs.

There are M thermal simulations, which are executed in parallel. Each of these thermal simulations represents a particle of the PSO, which is characterized by a set of parameters

$$p_m = \{R_{th1,m},\, C_{th1,m},\, R_{th2,m},\, C_{th2,m},\, R_{th3,m},\, C_{th3,m}\}\ \forall m \in [1,M] \tag{1}$$

describing a Cauer network with three RC elements between junction and ambient (Fig. 1). There are different execution rates in the virtual space, the one of the RTS $T_{exe,RTS}$ and that of the PSO $T_{exe,PSO}$. Depending on the considered converter it can be beneficial to have a higher execution rate for the electrical RTS $T_{exe,RTS,el}$ and a lower execution rate for the thermal RTS $T_{exe,RTS,th}$ to achieve higher accuracy with the limited computing capabilities. The performance of each particle is evaluated in each thermal RTS step based on the measured T_j and the junction temperature estimated by the particle $\hat{T}_{j,m}$. During one $T_{exe,PSO}$ period there are N executions at $T_{exe,RTS,th}$ and the PSO takes into account the average of the evaluations with the objective function:

$$f_{obj,m} = \frac{\sum_{n=1}^{N} \sqrt{(\hat{T}_{j,m,n} - T_{j,n})^2 + \frac{c_d}{s^{-2}} \left(\frac{\Delta \hat{T}_{j,m,n}}{T_{exe,RTS,th}} - \frac{\Delta T_{j,n}}{T_{exe,RTS,th}} \right)^2}}{N}\ \forall m \in [1,M]\ . \tag{2}$$

Herein c_d is the coefficient of the derivative part and for the implementation in the laboratory a filter needs to be applied to find the derivatives without distortion by the measurement noise.

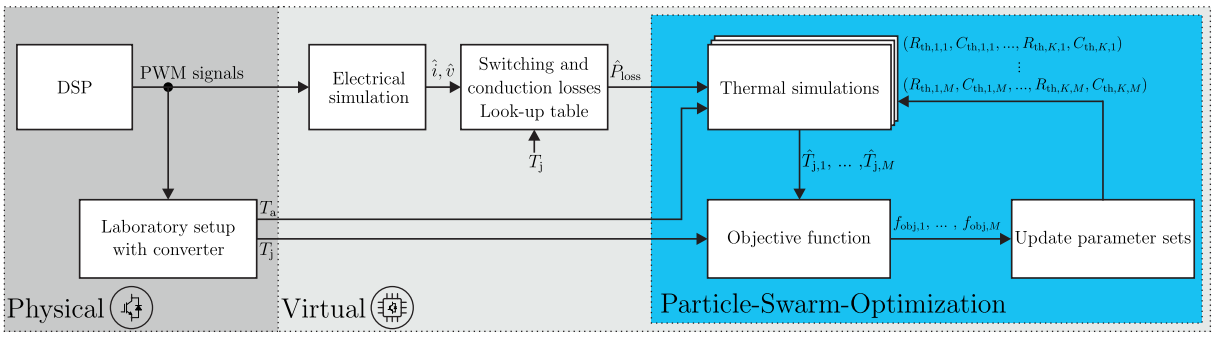

Fig. 2: Scheme of a PSO-based thermal DT.

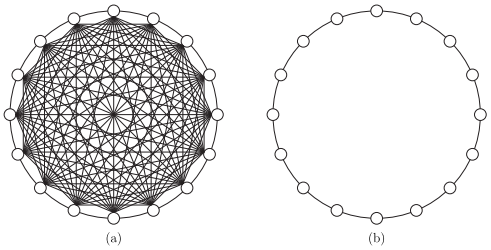

Fig. 3: Global topology (a) and local topology (b) for the PSO.

Table I: Coefficients and settings of the RTS and PSO in the real-time implementation.

Coefficient/Setting	Value
$T_{\text{exe,RTS,el}}$, $T_{\text{exe,RTS,th}}$	10 µs, 800 µs
$T_{\text{exe,PSO}}$	2 s
ω, c_1, c_2, c_3	0.7, 0.5, 0.5, 0.01
c_d, M	0.1, 16

Based on $f_{\text{obj},m}$ in this PSO execution and the best $f_{\text{obj},m}$ of previous PSO executions for each particle it is decided whether the particles best parameter set $p_{\text{best},m}$ should be updated or not. Further, there are different information topologies for the PSO (Fig. 3). In the global topology (Fig. 3 (a)) all particles are connected and converge towards the globally best parameter set g_{best} whereas in the local topology (Fig. 3 (b)) each particle is only connected with its neighbors and converges towards the locally best parameter set $l_{\text{best},m}$. The global topology provides faster convergence, but is prone to premature convergence, therefore the local topology is used in this work. The velocities of all dimensions of each particle v_m in step k of the PSO are calculated according to:

$$\begin{aligned} v_m(k) =& \omega v_m(k-1) + c_1 r_1 (p_{\text{best},m}(k-1) - p_m(k-1)) \\ &+ c_2 r_2 (l_{\text{best},m}(k-1) - p_m(k-1)) + c_3 r_3 p_m(k-1) \;\; \forall m \in [1, M] \; . \end{aligned} \tag{3}$$

Here ω is the inertia weight, r_1 and r_2 are randomly generated numbers between 0 and 1, r_3 is a randomly generated number between -1 and 1, and c_1, c_2, c_3 are coefficients of the PSO. Where, the first term multiplied with the coefficient c_1 describes the orientation on the best parameter set $p_{\text{best},m}$ the specific particle ever had, judged on the achieved objective function value. The second term multiplied with the coefficient c_2 orients on the parameter set $l_{\text{best},m}$ of the locally best neighbor particle. The last part multiplied with the coefficient c_3 inserts an own vibration of the particles, which prevents the swarm from getting stuck in local minima of the objective function. The parameters of each particle are updated by adding the velocity to the parameters of the last period:

$$p_m(k) = p_m(k-1) + v_m(k) \;\; \forall m \in [1, M] \; . \tag{4}$$

Real-Time Implementation

The capability of the thermal DT to find the proper Cauer network parameters is demonstrated based on a real-time simulation with a digital thermal reference model. This proof of concept is investigated with a simplified Cauer network, which describes the thermal behavior between a single junction, which

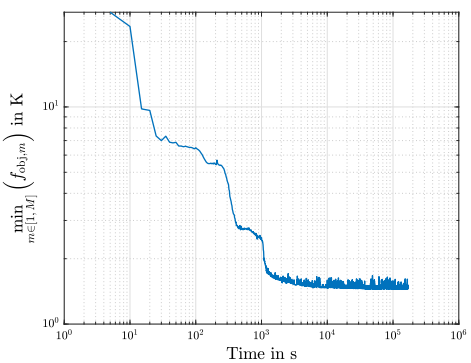

Fig. 4: Evolution of the objective function in the real-time implementation.

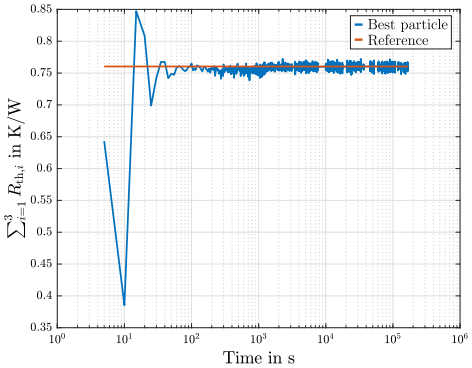

Fig. 5: Convergence of the sum of thermal resistances of the best particle in the real-time implementation.

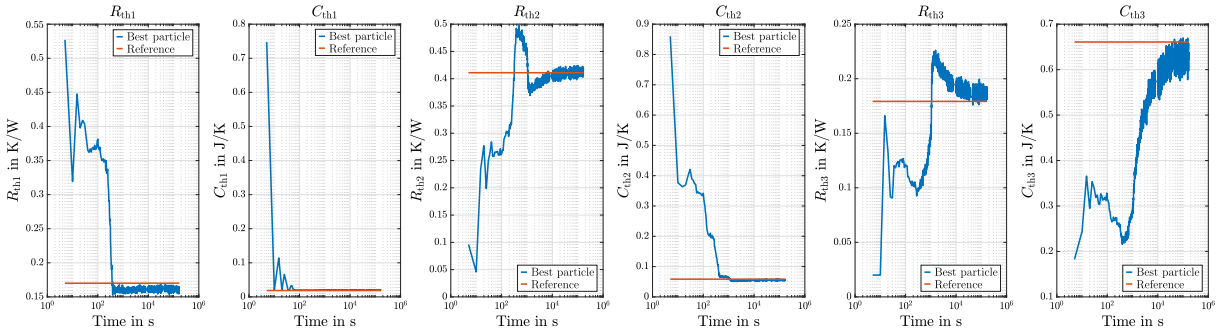

Fig. 6: Convergence of the Cauer network parameters of the best particle in the real-time implementation.

represents the IGBT and the diode of the buck converter, and the ambient temperature with three RC elements. A discussion on considering multiple heat sources is given in the second last section. The real-time simulation was executed on a Typhoon HIL402 system and the chosen coefficients and settings of the RTS and PSO are listed in table I. The converter is operated with a square-wave input for the duty cycle whose period is equal to $T_{\mathrm{exe,PSO}}$, so that one full thermal cycle is considered in each PSO step.

The evolution of the objective function (2) can be seen in Fig. 4. Herein, always the value of the best particle in each PSO step is used, this also applies for the parameters shown in the following. Among the parameters the fastest convergence can be achieved for the sum of thermal resistances (Fig. 5), because it has great influence on the average junction temperature, which affects the first part of the objective function (2) strongly. As it can be seen on the single parameters (Fig. 6), the closer the RC element is to the junction, the faster its parameters are converging, because changing them has a greater impact on the junction temperature. The parameters of the last RC element have only slight impact on the junction temperature and can only converge to the values of the thermal reference model after the other RC elements have already reached the values of thermal reference parameters.

Laboratory Results

The laboratory setup is shown in Fig. 7 and the connection scheme of the equipment in Fig. 9. Herein, the digital signal processor (DSP) (TMS320F28379D from Texas Instruments) provides the gate signals to the physical converter (with an open FP25R12KE3 power module from Infineon) and to the HIL system

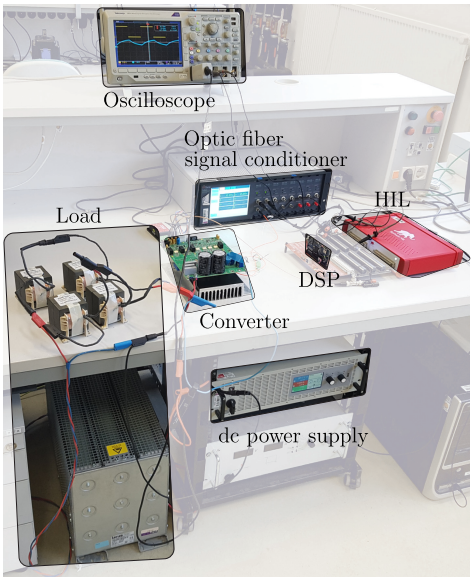

Fig. 7: Laboratory setup for thermal DT.

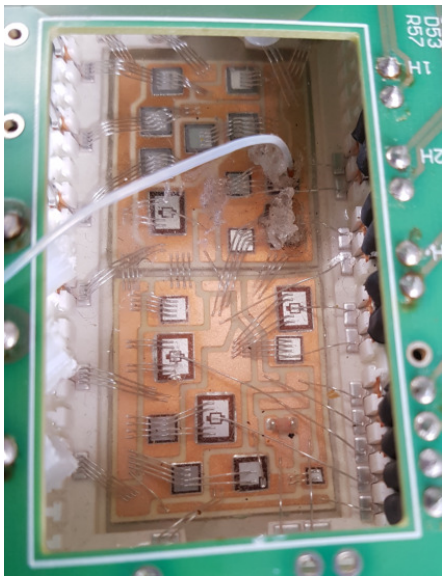

Fig. 8: Optic fiber temperature sensor placement in the open IGBT module.

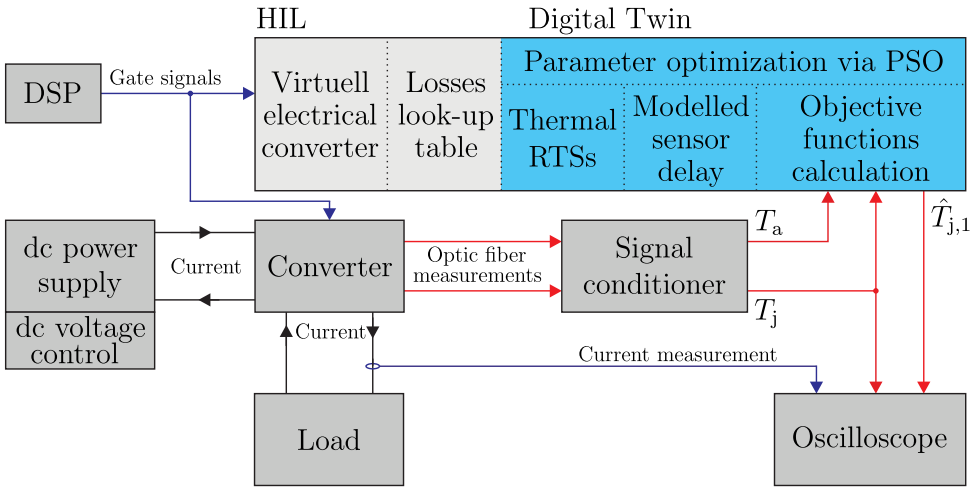

Fig. 9: Connection scheme of equipment in the laboratory setup.

(Typhoon HIL402), which executes the PSO-based thermal digital twin, at the same time. The converters dc link voltage of 200 V is controlled by the dc power supply (EA-PSI 9750-20 from Elektro-Automatik) and the converter feeds a load composed of a resistor (18 Ω) and an inductor (1.8 mH). The temperature of the IGBT in the open power module (Fig. 8) as well as the ambient temperature are measured with optic fiber temperature sensors (OTG-A from Opsens Solutions), which are connected to the optic fiber signal conditioner (PSC-D-N-N-N from Opsens Solutions). The signal conditioner scales the measured temperatures to voltages between −5 V and 5 V, which are given to the HIL system and scaled back to the temperatures there. The −5 V to 5 V scaled measured junction temperature as well as the estimated

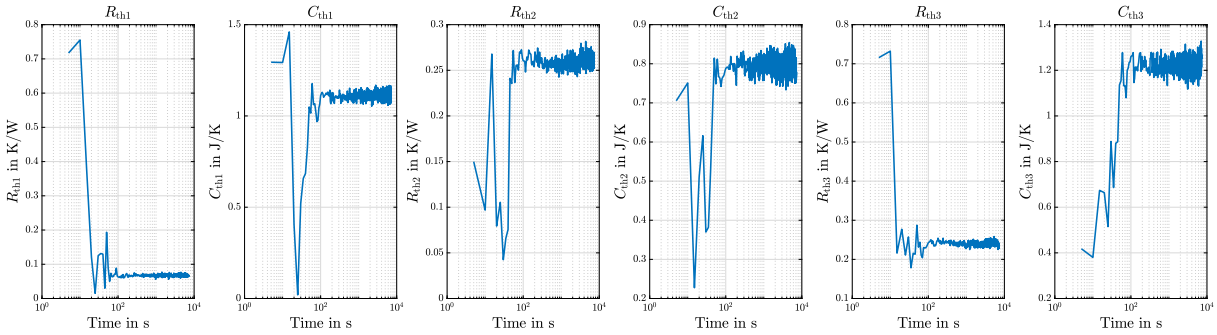

Fig. 10: Convergence of the Cauer network parameters of the best particle in the laboratory test.

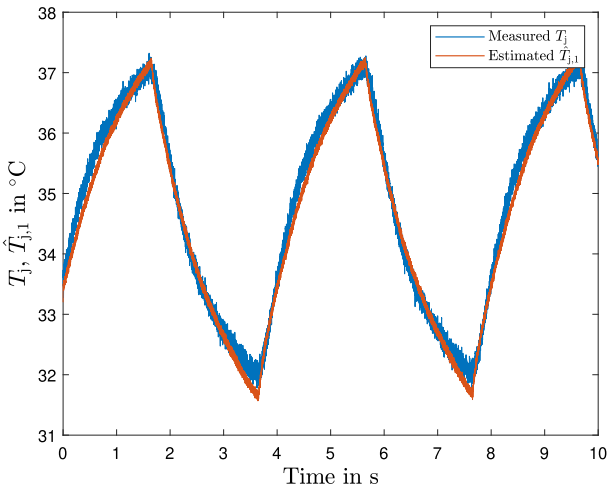

Fig. 11: Measured junction temperature (blue) and estimated junction temperature of particle one (red).

junction temperature of particle one are captured with an oscilloscope (DPO 3014 from Tektronix) and scaled back in Matlab afterwards. For the laboratory test the coefficients and settings of table I are used such as for the real-time implementation, except for a change in $T_{\mathrm{exe,PSO}}$ and accordingly the period for the square-wave input for the duty cycle to 4 s. The convergence of the parameters to a fixed parameter set in the laboratory test can be seen in Fig. 10. Herein, giving reference parameters is not possible because the real thermal behavior can never be fully captured by the model, however the PSO based DT adapts the parameters of the Cauer networks of all the particles to find the optimal representation of the real behavior by the model according to the objective function. The measured junction temperature and the estimated junction temperature of particle one after convergence to the fixed parameter set can be seen in Fig. 11.

Discussion of Field Application

A critical point for the usage of thermal digital twins in field applications is the need for modeling temperatures of multiple dies. As long as the heat dissipation of the different dies is coupled negligibly, the approach can be applied to each die independently. However, in semiconductor modules the thermal cross-coupling effects between the different dies are significant [19]. Therefore, the whole thermal network of all the dies, which considers the thermal cross-coupling between them, needs to be estimated by each of the particles of the PSO. An often used thermal model to consider cross-coupling effects is the linear accumulation of self heating and all cross-coupled heating by other dies [20–23]

$$\begin{bmatrix} \hat{T}_{\mathrm{j,I1}}(t) \\ \hat{T}_{\mathrm{j,D1}}(t) \\ \hat{T}_{\mathrm{j,I2}}(t) \\ \hat{T}_{\mathrm{j,D2}}(t) \end{bmatrix} = \begin{bmatrix} \dot{Z}^{\mathrm{I1}}_{\mathrm{th,self}}(t) & \dot{Z}^{\mathrm{I1}\leftarrow\mathrm{D1}}_{\mathrm{th,cross}}(t) & \dot{Z}^{\mathrm{I1}\leftarrow\mathrm{I2}}_{\mathrm{th,cross}}(t) & \dot{Z}^{\mathrm{I1}\leftarrow\mathrm{D2}}_{\mathrm{th,cross}}(t) \\ \dot{Z}^{\mathrm{D1}\leftarrow\mathrm{I1}}_{\mathrm{th,cross}}(t) & \dot{Z}^{\mathrm{D1}}_{\mathrm{th,self}}(t) & \dot{Z}^{\mathrm{D1}\leftarrow\mathrm{I2}}_{\mathrm{th,cross}}(t) & \dot{Z}^{\mathrm{D1}\leftarrow\mathrm{D2}}_{\mathrm{th,cross}}(t) \\ \dot{Z}^{\mathrm{I2}\leftarrow\mathrm{I1}}_{\mathrm{th,cross}}(t) & \dot{Z}^{\mathrm{I2}\leftarrow\mathrm{D1}}_{\mathrm{th,cross}}(t) & \dot{Z}^{\mathrm{I2}}_{\mathrm{th,self}}(t) & \dot{Z}^{\mathrm{I2}\leftarrow\mathrm{D2}}_{\mathrm{th,cross}}(t) \\ \dot{Z}^{\mathrm{D2}\leftarrow\mathrm{I1}}_{\mathrm{th,cross}}(t) & \dot{Z}^{\mathrm{D2}\leftarrow\mathrm{D1}}_{\mathrm{th,cross}}(t) & \dot{Z}^{\mathrm{D2}\leftarrow\mathrm{I2}}_{\mathrm{th,cross}}(t) & \dot{Z}^{\mathrm{D2}}_{\mathrm{th,self}}(t) \end{bmatrix} * \begin{bmatrix} P_{\mathrm{loss,I1}}(t) \\ P_{\mathrm{loss,D1}}(t) \\ P_{\mathrm{loss,I2}}(t) \\ P_{\mathrm{loss,D2}}(t) \end{bmatrix} + \begin{bmatrix} T_{\mathrm{a}} \\ T_{\mathrm{a}} \\ T_{\mathrm{a}} \\ T_{\mathrm{a}} \end{bmatrix} . \tag{5}$$

Each of these thermal impedances is typically described by a third- or fourth-order thermal network, which leads to a high number of parameters [24]. Having a high dimensional search area can impede the convergence of the PSO-based thermal DT algorithm. Thus, the approach would benefit from thermal models, which include cross coupling effects and provide a low number of parameters.

Conclusion

The thermal behavior of power semiconductors is highly important for assessing their state-of-health as well as for the implementation of measures to improve their reliability, such as active thermal control. This work proposed a Particle-Swarm-Optimization-based Digital Twin approach to extract the thermal impedance of power semiconductors for real-time applications. By using a digital reference model in a real-time simulation, it has been shown that the PSO-based thermal Digital Twin can find the parameters of a Cauer network with three RC elements. This proves that the approach is able to converge to thermal networks with possible physical meaning. The convergence of the algorithm to a fixed parameter set is validated in the laboratory and the estimation of the junction temperature after convergence is shown.

References

[1] F. Blaabjerg, R. Teodorescu, M. Liserre, and A. Timbus, "Overview of control and grid synchronization for distributed power generation systems," *IEEE Transactions on Industrial Electronics*, vol. 53, no. 5, pp. 1398–1409, 2006.

[2] H. Wang, M. Liserre, F. Blaabjerg, P. de Place Rimmen, J. B. Jacobsen, T. Kvisgaard, and J. Landkildehus, "Transitioning to physics-of-failure as a reliability driver in power electronics," *IEEE Journal of Emerging and Selected Topics in Power Electronics*, vol. 2, no. 1, pp. 97–114, 2014.

[3] J. Falck, C. Felgemacher, A. Rojko, M. Liserre, and P. Zacharias, "Reliability of power electronic systems: An industry perspective," *IEEE Industrial Electronics Magazine*, vol. 12, no. 2, pp. 24–35, 2018.

[4] M. Andresen, J. Kuprat, V. Raveendran, J. Falck, and M. Liserre, "Active thermal control for delaying maintenance of power electronics converters," *Chinese Journal of Electrical Engineering*, vol. 4, no. 3, pp. 13–20, 2018.

[5] S. Kalker, L. A. Ruppert, C. H. Van der Broeck, J. Kuprat, M. Andresen, T. A. Polom, M. Liserre, and R. W. De Doncker, "Reviewing thermal monitoring techniques for smart power modules," *IEEE Journal of Emerging and Selected Topics in Power Electronics*, pp. 1–1, 2021.

[6] J. Kuprat, C. H. van der Broeck, M. Andresen, S. Kalker, M. Liserre, and R. W. De Doncker, "Research on active thermal control: Actual status and future trends," *IEEE Journal of Emerging and Selected Topics in Power Electronics*, vol. 9, no. 6, pp. 6494–6506, 2021.

[7] F. Tao, H. Zhang, A. Liu, and A. Y. C. Nee, "Digital twin in industry: State-of-the-art," *IEEE Transactions on Industrial Informatics*, vol. 15, no. 4, pp. 2405–2415, 2019.

[8] Y. Peng, S. Zhao, and H. Wang, "A digital twin based estimation method for health indicators of dc-dc converters," *IEEE Transactions on Power Electronics*, vol. 36, no. 2, pp. 2105–2118, 2021.

[9] A. Wunderlich and E. Santi, "Digital twin models of power electronic converters using dynamic neural networks," in *2021 IEEE Applied Power Electronics Conference and Exposition (APEC)*, 2021, pp. 2369–2376.

[10] M. Milton, C. De La O, H. L. Ginn, and A. Benigni, "Controller-embeddable probabilistic real-time digital twins for power electronic converter diagnostics," *IEEE Transactions on Power Electronics*, vol. 35, no. 9, pp. 9850–9864, 2020.

[11] S. Chen, S. Wang, P. Wen, and S. Zhao, "Digital twin for degradation parameters identification of dc-dc converters based on bayesian optimization," in *2021 IEEE International Conference on Prognostics and Health Management (ICPHM)*, 2021, pp. 1–9.

[12] M. Musallam, C. Buttay, M. Whitehead, and M. Johnson, "Real-time compact electronic thermal modelling for health monitoring," in *2007 European Conference on Power Electronics and Applications*, 2007, pp. 1–10.

[13] M. Musallam and C. M. Johnson, "Real-time compact thermal models for health management of power electronics," *IEEE Transactions on Power Electronics*, vol. 25, no. 6, pp. 1416–1425, 2010.

[14] H. Chen, B. Ji, V. Pickert, and W. Cao, "Real-time temperature estimation for power mosfets considering thermal aging effects," *IEEE Transactions on Device and Materials Reliability*, vol. 14, no. 1, pp. 220–228, 2014.

[15] T. K. Gachovska, B. Tian, J. L. Hudgins, W. Qiao, and J. F. Donlon, "A real-time thermal model for monitoring of power semiconductor devices," *IEEE Transactions on Industry Applications*, vol. 51, no. 4, pp. 3361–3367, 2015.

[16] W. Wang, H. R. Wickramasinghe, K. Ma, and G. Konstantinou, "Real-time co-simulation for electrical and thermal analysis of power electronics," in *2019 9th International Conference on Power and Energy Systems (ICPES)*, 2019, pp. 1–5.

[17] L. Felsberger, B. Todd, and D. Kranzlmueller, "Power converter maintenance optimization using a model-based digital reliability twin paradigm," in *2019 4th International Conference on System Reliability and Safety (ICSRS)*, 2019, pp. 213–217.

[18] B. Rodriguez, E. Sanjurjo, M. Tranchero, C. Romano, and F. Gonzalez, "Thermal parameter and state estimation for digital twins of e-powertrain components," *IEEE Access*, vol. 9, pp. 97 384–97 400, 2021.

[19] A. Stippich, M. Neubert, A. Sewergin, and R. W. De Doncker, "Significance of thermal cross-coupling effects in power semiconductor modules," in *2016 IEEE 2nd Annual Southern Power Electronics Conference (SPEC)*, 2016, pp. 1–6.

[20] B. Zahn, "Steady state thermal characterization of multiple output devices using linear superposition theory and a non-linear matrix multiplier," in *Fourteenth Annual IEEE Semiconductor Thermal Measurement and Management Symposium (Cat. No.98CH36195)*, 1998, pp. 39–46.

[21] U. Drofenik, D. Cottet, A. Müsing, J.-M. Meyer, and J. W. Kolar, "Modelling the thermal coupling between internal power semiconductor dies of a water-cooled 3300v/1200a hipak igbt module," in *Proceedings of Power Conversion and Intelligent Motion Conference*, 2007, pp. 1–8.

[22] A. S. Bahman, K. Ma, and F. Blaabjerg, "Thermal impedance model of high power igbt modules considering heat coupling effects," in *2014 International Power Electronics and Application Conference and Exposition*, 2014, pp. 1382–1387.

[23] M. Shahjalal, M. R. Ahmed, H. Lu, C. Bailey, and A. J. Forsyth, "An analysis of the thermal interaction between components in power converter applications," *IEEE Transactions on Power Electronics*, vol. 35, no. 9, pp. 9082–9094, 2020.

[24] Y. Zhang, Z. Wang, H. Wang, and F. Blaabjerg, "Artificial intelligence-aided thermal model considering cross-coupling effects," *IEEE Transactions on Power Electronics*, vol. 35, no. 10, pp. 9998–10 002, 2020.